

Neuroprotective effects of celastrol on sciatic nerve transection model in male Wistar rats

Haider F. Al-Saedi¹, Hussein A. Ghanimi², Seyedeh Mahdiah Khoshnazar³, Mohammad B. Ghayour⁴, Arash Abdolmaleki^{5*}

¹ College of Pharmacy, University of Al-Ameed, Karbala, Iraq

² College of Nursing, University of Al-Ameed, Karbala, Iraq

³ Neuroscience Research Center, Institute of Neuropharmacology, Kerman University of Medical Sciences, Kerman, Iran

⁴ Department of Biology, Faculty of Science, Ferdowsi University of Mashhad, Mashhad, Iran

⁵ Department of Biophysics, Faculty of Advanced Technologies, University of Mohaghegh Ardabili, Namin, Iran

ARTICLE INFO

Article type:
Original

Article history:
Received: Jul 7, 2022
Accepted: Sep 5, 2022

Keywords:
Celastrol
Cytokine
Inflammation
Macrophage
Sciatic nerve

ABSTRACT

Objective(s): Celastrol is an herbal compound with neuroprotective properties. Our research aimed to assess the neuroprotective properties of celastrol on sciatic nerve transection in rats.

Materials and Methods: The rats' left sciatic nerve was cut and sutured directly. The animals were then given 1 or 2 mg/kg celastrol intraperitoneally for two weeks. The sensory and locomotor behaviors of the animals were then evaluated for 16 weeks. Immunohistochemistry, ELISA, and real-time PCR were also utilized to evaluate macrophage polarization, cytokine secretion, and neurotrophin expression in injured nerves.

Results: Results showed that both doses of celastrol significantly accelerated nerve regeneration and improved sensorimotor functional recovery when compared with controls. Nevertheless, administration of 2 mg/kg of celastrol significantly outperforms treatment with a dose of 1 mg/kg. Celastrol treatment-induced M2 polarization in macrophages decreased proinflammatory cytokines at the injury site. It also increased the expression of BDNF mRNA.

Conclusion: These findings suggest that a two-week treatment with celastrol had neuroprotective effects in a rat sciatic nerve transection model, most likely by inducing macrophage M2 polarization and anti-inflammatory effects.

► Please cite this article as:

Al-Saedi HF, Ghanimi HA, Khoshnazar SM, Ghayour MB, Abdolmaleki A. Neuroprotective effects of celastrol on sciatic nerve transection model in male Wistar rats. *Iran J Basic Med Sci* 2022; 25: 1251-1259. doi: <https://dx.doi.org/10.22038/IJBMS.2022.66614.14617>

Introduction

Peripheral nerve injuries (PNIs) are the leading cause of morbidity with significant socioeconomic consequences (1, 2). Functional restoration after severe PNI is always incomplete because current treatments are insufficient, even in the ideal setting (3). Following a PNI (axonotmesis or neurotmesis), a cascade of cellular events transforms injured neurons and Schwann cells into regenerative cells (4). The surviving axons in the proximal nerve stump retract behind the injury site while the distal axons undergo Wallerian degeneration, allowing for axonal regeneration (1, 5). However, complete Wallerian degeneration and successful nerve regeneration require involvement of Schwann cells and immune cells, particularly macrophages (6, 7). Macrophages are considered a therapeutic target for PNI management because they play an important role in nerve regeneration via cellular debris clearance and cytokine secretion (8, 9). Macrophages in the distal nerve stump have both pro-inflammatory (M1) and anti-inflammatory (M2) phenotypes and the M2 macrophage phenotype has four subtypes (10, 11). The M1 phenotype stimulates Schwann cell proliferation and transdifferentiation into the regenerative phenotype (12). This phenotype is then transformed into the pro-healing M2 phenotype and contributes to nerve regeneration. (1, 13). As a result, promoting the polarization of M1 phenotypes toward M2 phenotypes is an important phase in peripheral nerve regeneration (14, 15). Despite the importance of

macrophages in nerve regeneration, the therapeutic potential of macrophage modulation has received little consideration. It seems that anti-inflammatory agents promoting macrophages to the M2 phenotype could be a useful tool for promoting peripheral nerve regeneration (1).

Celastrol, a pentacyclic triterpenoid isolated from *Tripterygium wilfordii* root, has been shown to reduce macrophage inflammation by polarizing them toward a pro-healing (M2) phenotype (16-19). Furthermore, some studies suggest that celastrol has antioxidative and metabolism-remodeling properties (20). Animal studies have also confirmed its neuroprotective properties against cerebral ischemia and retinal ganglion cell injuries (21, 22). However, the effect of celastrol on PNI remains unclear. As a result, the purpose of this study was to determine the neuroprotective effects of celastrol on PNI in male Wistar rats. We also investigate the celastrol effects on macrophage polarization.

Materials and Methods

Animals and ethics statement

This study included 72 adult male Wistar rats weighing between 200–250 g. Animals were kept in Plexiglas cages under a standard lab environment (humidity 60 ± 5%, temperature, 22±2 °C, and 12-hour light cycles), with free access to food and tap water. All animal experiments

*Corresponding author: Arash Abdolmaleki. Department of Biophysics, Faculty of Advanced Technologies, University of Mohaghegh Ardabili, Namin, Iran. Email: Abdolmalekiarash1364@gmail.com

were carried out according to the guidelines of the Ethics Committee of the Mohaghegh Ardabili University of Ardabil (Iran).

Surgical method

This study considered the therapeutic properties of celestrol on sciatic nerve transection (SNT). The surgeries were carried out under aseptic conditions by a single surgeon using a surgical microscope (Zeiss, Germany). Animals were given anesthesia by intraperitoneal injection of ketamine (80 mg/kg) and xylazine (15 mg/kg). The left sciatic nerve was transected 15 mm superior to the bifurcation into the common fibular and tibial nerves. Then, the proximal and distal nerve stumps were reconnected with four epineurial micro sutures immediately (10-0 nylon, Ethicon). Subsequently, the muscle and skin were closed using 6-0 prolene (Ethicon) and 4-0 nylon (Ethilon) sutures, respectively. Finally, the rats were permitted to recover from anesthesia. As an analgesic, subcutaneous buprenorphine was administered to the operated animals (0.05 mg/kg). Furthermore, bitter nail polish was also administered to the operated limb to prevent autotomy (23, 24).

Experimental groups and animal treatment

Fifty-four rats with left SNT were randomized to three groups (n = 18), including the control group (1% dimethyl sulfoxide in 0.9% saline solution), 1 mg/kg celestrol treated group, and 2 mg/kg celestrol treated group. The doses of celestrol were chosen based on previous research (25, 26). In the sham-operation group, 18 rats underwent the surgical procedure without nerve injury. The sham-treated rats served as healthy nerve controls. Celestrol or an equal volume of the celestrol vehicle was daily administered via intraperitoneal injections within 14 days after surgery. Celestrol was dissolved in 1% dimethyl sulfoxide in a 0.9% saline solution. Similarly, the control group received an equal volume of vehicles. At the end of the experiment, all the animals were euthanized by inhalation of CO₂, and their bodies were burned in a furnace.

Walking track analysis

Walking track analysis, followed by Sciatic Functional Index (SFI) calculation, was used to evaluate locomotor activity at 2, 4, 8, 12, and 16 weeks after surgery. Rats with black ink-painted hind limbs were permitted to walk down the white sheet-covered corridor (50 cm × 10 cm) to leave footprints. Thereafter, the distance between the third toe and the hind limb pads (paw length, PL), the distance between the first and fifth toes (toe spread, TS), and the distance between the second and fourth toes (intermediary toe spread, ITS) in the healthy (N) and wounded (E) hind limbs were measured. The footprint parameters were then entered into the Bain *et al.* (1989) formula: $SFI = -38.3 [(EPL-NPL)/NPL] + 109.5 [(ETS-NTS)/NTS] + 13.3 [(EIT-NIT)/NIT] - 8.8$ (27). SFI scores vary from 0 to -100, with 0 implying normal function and -100 representing severe hindlimb motor impairment. A score of -100 was assigned when there was no measurable footprint. Finally, a blind operator reported three footprints on average for each animal (28, 29).

Hot plate test

The thermal withdrawal reflex latency (WRL) for the operated leg (thermal nociception threshold) was measured using a hot plate test to assess sensory function. Rats were restrained and placed on a hot plate at 55 ± 1 °C (PE34, IITC Life Sciences, USA) with their hind paw. The time between the start of the hotplate touch and the WRL was

recorded. All assays were repeated three times at two-minute intervals, with the averages given. We set the cut-off time at 12 sec to avoid foot tissue injury (30).

Electrophysiological evaluation

In the 16th week postoperatively, we measured the compound muscle action potential (CMAP) and motor nerve conduction velocity (NCV) under anesthesia. The nerve was exposed, and a fine bipolar hook electrode was positioned 5 mm proximal to the anastomosis site. The recording and ground electrodes were inserted into the rat's gastrocnemius muscle belly and tail. Furthermore, a reference electrode was positioned between the recording and stimulating electrodes. The CMAP amplitude was calculated from the baseline to the max negative point, and response latency was calculated from the stimulus signal to the first negative deviation. All CMAPs were amplified and displayed on a digital oscilloscope. To measure MNCV, the sciatic nerve was stimulated 5 mm proximally or 10 mm distally to the anastomosis area, and CMAPs were recorded from the gastrocnemius muscle. The MNCV was then calculated by dividing the length between the two stimulation points by the difference in CMAP latency. On the uninjured contralateral limbs, the normal CMAP and MNCV were recorded (31). In addition, we used a heating pad to keep body temperature around 36 °C to avoid CMAP variations.

Histomorphometry analysis

Histomorphometry was used to quantify regenerating nerve morphology in the 16th postoperative week. Under anesthesia, nerves were harvested carefully 5 to 10 mm distal to the anastomosis site. The nerves were then fixed overnight in 4% paraformaldehyde at 4 °C. Following that, the tissue specimens were post-fixed in 1% osmium tetroxide for 3 hr before being dehydrated in increasing concentrations of ethyl alcohol and embedded in paraffin. Finally, the specimens were cut into 1 µm-thick slices and subjected to 1% toluidine blue staining for light microscopy (Carl Zeiss, Germany) analysis. Utilizing the Image J software (National Institutes of Health, Maryland, USA), a blinded observer measured axon counts, axon diameter, myelin thickness, fiber diameter, and fiber G-Ratio. It is worth mentioning that the G-ratio is the ratio of the axonal diameter to the myelinated fiber diameter of the myelin sheath of a myelinated axon which is used as a structural index of optimal axonal myelination. The sciatic nerve of the uninjured contralateral limb was considered a healthy control (32).

Gastrocnemius muscle mass ratio

The mass ratio of the gastrocnemius muscle, the large muscle innervated by the sciatic nerve, was measured to determine nerve re-innervation and muscle atrophy. Following the electrophysiological evaluation, both limb gastrocnemius muscles were harvested and the moist muscle weight was immediately measured. The muscle mass ratio was then calculated by dividing the muscle weight on the operated side (left) by the muscle weight on the uninjured contralateral side (right). A ratio value closer to one indicates less muscle atrophy and better reinnervation (33, 34).

Masson trichrome staining

Muscle atrophy in the operated limb was assessed using Masson's trichrome staining. The harvested gastrocnemius muscles were fixed in paraformaldehyde and dehydrated in rising ethyl alcohol concentrations. After being cleared

with xylene, the nerve samples were embedded in paraffin and then sliced into 5 μm longitudinal sections. The specimens were then subjected to Masson's trichrome for light microscopy (Carl Zeiss, Germany). Image-Pro Plus 6.0 software was used to capture digital images and calculate muscle fiber areas. The uninjured contralateral muscle served as healthy control (35, 36).

Immunohistochemical staining

Immunohistochemical staining was performed three weeks after surgery to identify the total number of macrophages, pro-inflammatory macrophages (M1), and pro-healing macrophages (M2) in regenerating nerves. Four animals from each group were perfused using cold phosphate-buffered saline (PBS, pH = 7.4) (Merck, Germany), and the sciatic nerves were harvested 5 to 10 mm distal to the anastomosis site. The samples were fixed in 4% paraformaldehyde (Merck, Germany) and kept in a 30% sucrose (Merck, Germany) solution for 24 hr. Nerve specimens were then embedded in the Tissue-Tek OCT compound (Sakura, Japan) and cryosectioned. The 10 μm -thick transverse slices were treated for 1 hr in a blocking solution of goat serum (Gibco) in PBS at room temperature. Then, the slices were treated overnight at 4 °C with the following primary antibody solutions: CD68 (1:100, mouse IgG1, AbD Serotec (ED1)) to determine the total activated macrophages, CCR7 (1:200, rabbit, IgG, Cell Application) to identify the M1 macrophages and CD206 (1:100, rabbit, IgG, Santa Cruz Biotechnology) to identify the M2a and M2c macrophages. The nerve specimens were incubated for another 1 hour in a secondary antibody solution containing 0.5% Triton X-100 (Merck, Germany) in PBS. Eventually, the specimens were washed in PBS, coverslipped, and observed with a fluorescence microscope (Axioskop 2, Zeiss) (37).

Real-time polymerase chain reaction (real time-PCR)

The mRNA expression levels of neurotrophic factors (NGF, BDNF) were quantified by real-time PCR. Total RNA was extracted from nerve tissues with Trizol (Invitrogen) and then purified with the RNeasy Mini Kit (Qiagen). The quantity and purity of RNA samples were estimated using a Nanodrop ND-1000 spectrophotometer (Thermo Fisher Scientific) to measure absorbance at 260 nm (A260) and A260/A280 ratios. Total RNA (20 ng) was reverse transcribed into cDNAs by the Moloney murine leukemia virus (M-MLV) reverse transcriptase enzyme (Sigma-Aldrich). The Corbett thermal cycler (Corbett Research, Australia) was then used to amplify cDNA (20 ng) in the presence of forward and reverse primers (10 μM) and 2X Power SYBR Green Master Mix (5 μl ; Invitrogen) in 10 μl -reaction volume. The thermocycler program was as follows: pre-denaturation at 95 °C for 5 min, 35 cycles of denaturation at 94 °C for 30 sec, annealing at 57 °C for 20 sec, elongation at 72 °C for 30 sec, and final elongation at 72 °C for 5 min. All assays were run in triplicate, and the target gene expression was normalized using the internal control glyceraldehyde 3-phosphate dehydrogenase (GAPDH). The relative changes in gene expression were determined by the $2^{-\Delta\Delta\text{Ct}}$ method. Primer sequences used for NGF were F: CAGAGTTTTGGCCTGTGGTC and R: GGACATTACGCTATGCACCTC; for BDNF were F: AGCGCGAATGTGTTAGTGGT and R: GCAATTGTTGCCTCTTTTCT; and for GAPDH were F: TGGGAAGCTGGTCATCAAC and R: GCATCACCCATTGATGTT, as previously described by Maeda and colleagues (38).

Enzyme-linked immunosorbent assay (ELISA)

Seven days after surgery, we used an ELISA assay to measure pro-inflammatory cytokine levels (TNF- α , IL-1 β , IL-6) in the transected sciatic nerves. The sciatic nerves (5 mm of proximal and distal nerve stumps) were harvested and homogenized in a cocktail of Tris buffer, protease inhibitors (Roche, Germany), and phosphatase inhibitors (Roche, Germany). Subsequently, the homogenized tissue was centrifuged at 15,000 RPM for 20 min, and the supernatants were collected. The supernatants were used for the measurement of TNF- α , IL-1 β , and IL-6 concentrations using ELISA kits for rats (R & D Systems Inc., MN, USA). Following the primary and secondary antibodies binding, the substrate and stop solutions were added to the wells. The intensity of the color reflected the amount of cytokine concentration. Cytokine concentrations were quantified as pg/mg total protein using a standard curve (39, 40).

Statistical analysis

SPSS Statistics 20.0 was used to analyze the data (SPSS Inc., Chicago, Illinois, USA). The Shapiro-Wilk test was employed to determine the data's normality. The statistically significant differences between groups were determined using a one-way analysis of variance (ANOVA). A Tukey *post hoc* analysis was used to compare the groups. Data were shown as the mean \pm standard deviation (SD), with $P < 0.05$ considered statistically significant.

Results

All operated animals survived until the end of the experiment. However, due to autotomy, one animal from the control group was euthanized with CO₂ inhalation. Besides, there was no apparent neuroma formation or inflammatory reaction.

SFI

A flaccid operated foot was present in all animals with SNT. Before surgery, the mean SFI score in all groups ranged from -3.4 to -5.6, indicating normal function (Figure 1). Nevertheless, four weeks after SNT, the mean SFI scores decreased dramatically to the lowest level (< -70) in all animals, without any significant difference between groups.

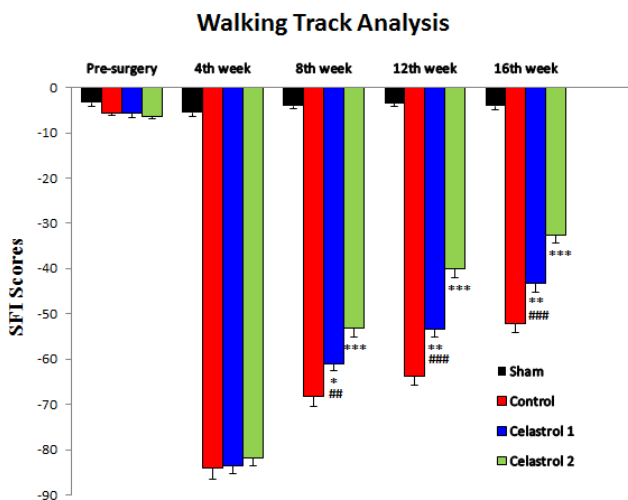


Figure 1. Average sciatic function index (SFI) values in the 4th, 8th, 12th, and 16th week following surgery of sciatic nerve in all groups. Data were expressed as mean \pm SD (n = 10). * $P < 0.05$, ** $P < 0.01$ and *** $P < 0.001$ vs control group, and ## $P < 0.01$ and ### $P < 0.001$ vs celastrol (2 mg/kg) group

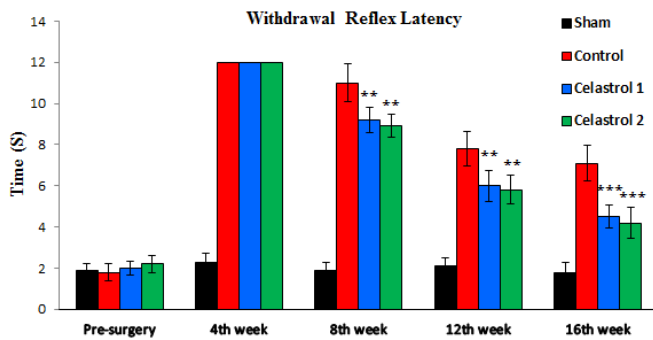


Figure 2. Effect of celestrol on thermal nociception 4th, 8th, 12th, and 16th week after surgery of sciatic nerve in all groups. Data were expressed as mean \pm SD (n=10). * P <0.05, ** P <0.01 and *** P <0.001 vs control group

Afterward, SFI scores significantly increased at different rates in all animals with SNT, confirming nerve regeneration and muscle reinnervation (Figure 1). However, the 2 mg/kg celestrol group revealed a significantly higher mean SFI value than that of the 1 mg/kg celestrol and control groups in the 8th, 12th, and 16th weeks after surgery (P <0.01). Similarly, the mean SFI score of the 1 mg/kg celestrol-treated rats was also superior to the control group in the 8th, 12th, and 16th weeks post-operative, as shown in Figure 1 (P <0.05). Sham surgery did not affect the normal SFI value significantly.

Hot plate

Four weeks post-surgery, the WRL in all animals increased dramatically to the cut-off value of 12 sec, indicating severe sensory impairment (Figure 2). However, the thermal nociceptive threshold improved markedly over time, and the WRL in the 1 and 2 mg/kg celestrol groups declined to 4.5 ± 0.55 sec and 4.2 ± 0.78 sec at the end of the 16th week, respectively. Statistical analysis revealed no significant difference between the two celestrol treatment groups, but the WRL in these groups was significantly lower than in controls in the 8th, 12th, and 16th weeks after surgery (P <0.01). As a result, celestrol treatment could improve sensory function retrieval in rats with sciatic nerve defects.

Electrophysiological evaluation

At the 16th week postoperatively, an electrophysiological assessment was performed to qualify motor fiber regeneration and muscle reinnervation. As shown in Figure 3A, CMAPs were detected as a gradual increase pattern in all SNT rats from the fourth to the sixteenth week after surgery, indicating steady progress in nerve regeneration

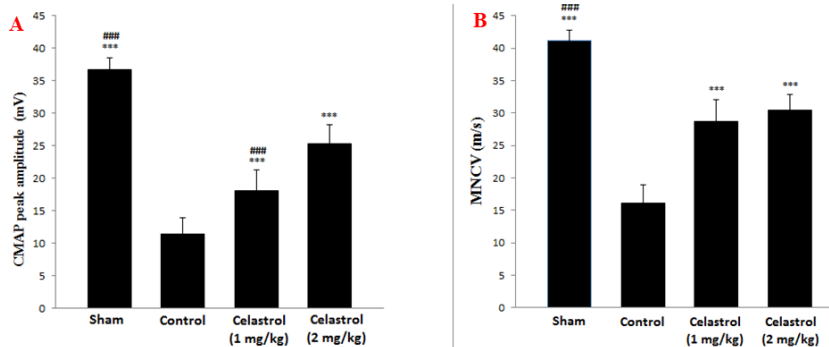


Figure 3. Electrophysiological evaluation of the regenerated nerves in rats with SNT at 16th-week post-surgery. (A) Representative results of CMAP amplitude after proximal stimulation of operated sciatic nerves. (B) MNCV values. Data were expressed as mean \pm SD (n = 10). *** P <0.001 vs control group, and ### P <0.001 vs celestrol (2 mg/kg) group

SNT: Sciatic nerve transection; CMAP: Compound muscle action potential

and functional recovery. The average of CMAPs peak amplitude and MNCV in rats given 1 mg/kg celestrol was 18.1 ± 3.1 mV and 28.7 ± 3.3 ms, respectively, and 25.3 ± 2.9 mV and 30.4 ± 2.4 ms in those given 2 mg/kg celestrol (Figure 3A and 3B). In accordance with the SFI results, the mean CMAP amplitude of rats treated with 2 mg/kg celestrol was significantly higher than that of rats given 1 mg/kg celestrol (Figure 3A; P <0.001). MNCV, on the other hand, increased gradually following SNT in rats, although it remained lower than in sham surgery. The mean MNCV was also increased in the 2 mg/kg celestrol group compared with the 1 mg/kg celestrol group, although this increase was not statistically significant (Figure 3B). Similarly, both electrophysiological parameters were significantly greater in celestrol-treated animals than in controls (P <0.05).

Histomorphometry analysis

At the end of the follow-up, histomorphometry was performed on sciatic nerves 5–8 mm distal to the nerve coaptation site to quantify axonal regeneration. Toluidine blue staining of the sciatic nerve in the control group revealed degraded myelin sheaths and decreased axon diameter as compared with the sham group (Figure 4). Similarly, the morphometric analysis showed that all rats with SNT had significantly higher myelinated axon counts, denser fiber distribution, smaller axonal diameter, lower myelin thickness, and improved G-ratio compared with the

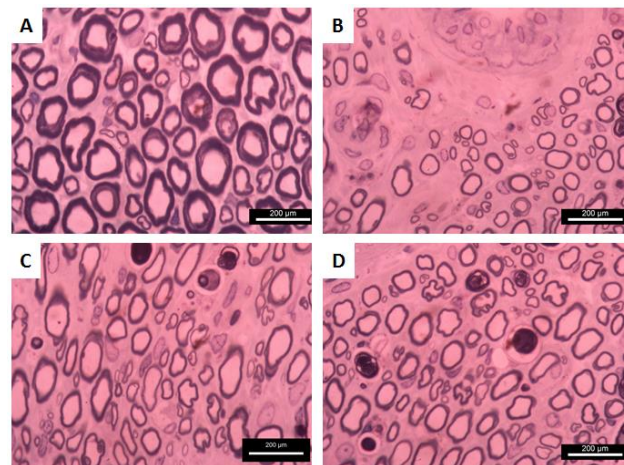


Figure 4. Toluidine blue staining of regenerated nerves at the end of the experiment. (A) Sham group (B) control group (C) celestrol (1 mg/kg), and (D) celestrol (2 mg/kg) (Scale bar: 200 μ m)

Table 1. Histomorphometry analysis of myelinated axons in regenerated sciatic nerve cross-sections at the 16th post-operative week

	Axon diameter	Myelin thickness	Fiber diameter	Myelinated fiber count	G-Ratio
Sham	4.65±0.4 *** ###	1.23±0.19 *** #	7.11±0.78 *** ###	7290±9768 * ###	0.65
Control	1.79±0.43 ###	0.64±0.12 ###	3.07±0.67 ###	8192±927 ###	0.58
Celastrol 1 mg/kg	2.8±0.41 **	0.85±0.27***	4.5±0.95 **	9271±1519* #	0.62
Celastrol 2 mg/kg	3.03±0.32 ***	0.9±0.16 ***	4.83±0.64 ***	10749±1066 ***	0.63

Values are shown as mean ± SD (n = 10). **P*<0.05, ***P*<0.01, and ****P*<0.001 for comparison with control group, and # *P*<0.05 and ### *P*<0.001 for comparison with celastrol (2 mg/kg) group

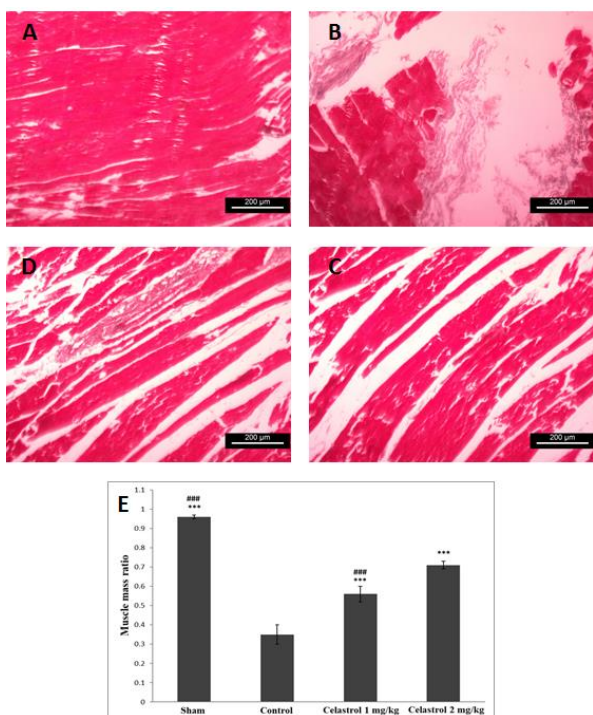


Figure 5. Gastrocnemius muscle atrophy measurement of all groups following surgery (A-D) Light micrograph of gastrocnemius muscle longitudinal sections stained with Masson trichrome at the 16th post-operative week. (A) sham operation, (B) control, (C) celastrol (1 mg/kg), and (D) celastrol (2 mg/kg) groups. (E) average gastrocnemius muscle mass ratio (operated/non-operated) in experimental groups. The data are shown as mean ± SD (n=10). ****P*<0.001 vs control group and ### *P*<0.001 vs celastrol (2 mg/kg) group

normal nerve in the sham surgery group (Table 1). On the other hand, rats given 2 mg/kg celastrol had a significant increase in the number of myelinated axons compared with those treated with 1 mg/kg celastrol, as shown in Table 1 (*P*<0.001). However, no significant difference was found between the two celastrol-treated groups in terms of axon diameter, myelin thickness, and G-ratio. Moreover, all morphometric parameters in rats treated with celastrol (1 mg/kg) were significantly superior to controls (*P*<0.001).

Gastrocnemius muscle atrophy

Muscle mass ratio and Masson's trichrome staining were employed 16 weeks after surgery to assess gastrocnemius atrophy. The muscle mass ratio was expressed as a percentage of the uninjured contralateral side. As illustrated in Figure 5E, all animals with SNT had gastrocnemius muscle atrophy and fiber degradation compared with the sham surgery group. However, celastrol treatment at both doses could significantly reduce muscle atrophy and increase muscle

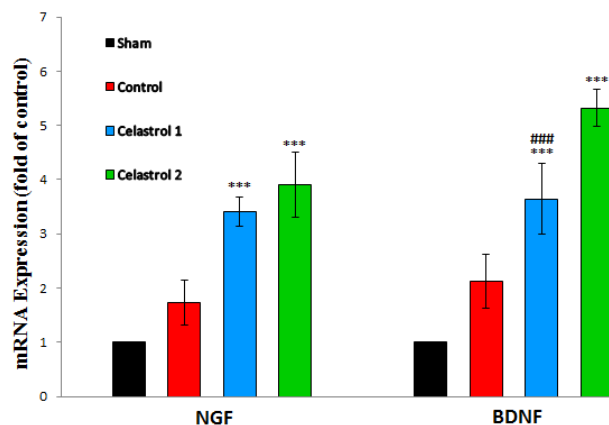


Figure 6. Effects of celastrol on NGF and BDNF mRNA expression in the sciatic nerve of rats with SNT. mRNA level in naive rats has been ascribed a value of 1, and the vertical axis numbers indicate relative changes from this baseline for each group. The data are shown as mean ± SD (n = 4). ****P*<0.001 vs control group and ### *P*<0.001 vs celastrol (2 mg/kg) group

mass ratio compared with the control group. Furthermore, rats given 2 mg/kg celastrol (0.56±0.04) had a significantly higher muscle mass ratio than those given 1 mg/kg celastrol (0.71±0.02) (see Figure 5E; *P*<0.001).

Masson's trichrome staining, on the other hand, revealed that the normal gastrocnemius muscle contained few fibrous connective fibers between muscle bundles (Figure 5A). Denervated muscles in rats with sciatic nerve deficits, on the other hand, had more fibrous connective tissues and higher muscle fiber degradation (Figure 5B-C). In the 16 weeks after surgery, the celastrol treatment improved the gastrocnemius muscle atrophy compared with controls. The results showed that rats who were given 2 mg/kg celastrol had less muscle atrophy and fibrous connective tissues than those given 1 mg/kg celastrol (Figure 5B and D).

The ratio of M1 to M2 macrophages in sciatic nerve

Three weeks following surgery, nerve tissues were immunostained for CD68, CCR7, and CD206 markers to assess the effect of celastrol on macrophage polarization. As shown in Figure 6, both CD206+ (M2a and M2c) and CCR7+ (M1) macrophages were detectable in all experimental groups. However, celastrol treatment did not affect the total number of macrophages, significantly. In contrast, immunohistochemical staining revealed that celastrol treatment at both doses could induce macrophage polarization from pro-inflammatory M1 to pro-healing M2 phenotype (Figure 6) and increased the CD206+/CD68+ ratio compared with controls (Figure 6; *P*<0.01). In this regard, rats given 2 mg/kg celastrol performed better than rats given 1 mg/kg celastrol (*P*<0.001). The CD206+/CD68+

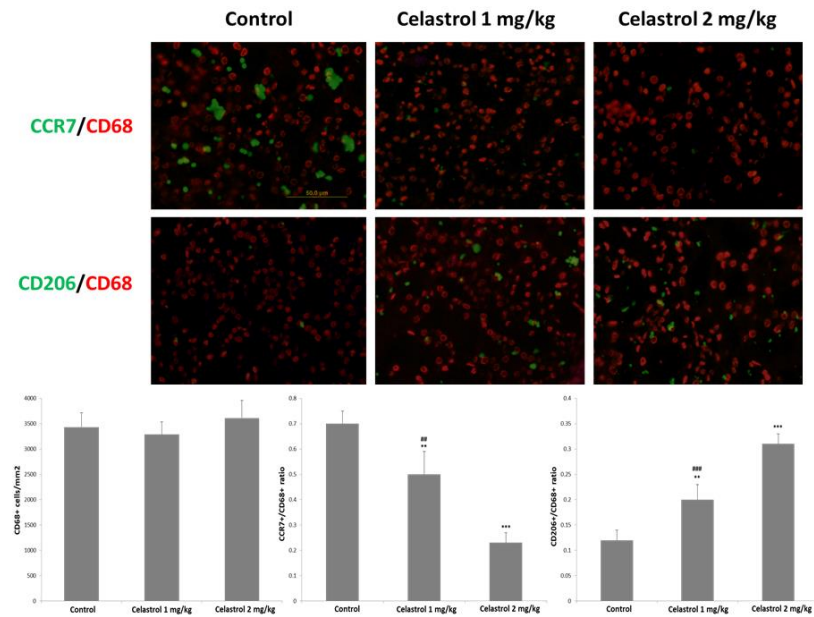


Figure 7. Effect of celestrol treatment on macrophage polarization in rats with SNT sciatic nerve. (A) Representation of double immunofluorescent staining of sciatic nerve resident macrophages with the M0 marker (CD68/red), M1 marker (CCR7/green), and M2 marker (CD206/green). (B) Quantitative analysis of the macrophage number. (C) Ratio of the pro-inflammatory phenotype to the CD68+ macrophages. (D) Ratio of the pro-healing phenotype to the CD68+ macrophages. The data are shown as mean ± SD (n = 4). ***P*<0.01 and ****P*<0.001 vs control group, and ## *P*<0.01 and ### *P*<0.001 vs celestrol (2 mg/kg) group SNT: Sciatic nerve transection

ratio was also significantly higher in rats given 1 or 2 mg/kg celestrol than in controls. These findings revealed that M2 macrophages outnumbered M1 macrophages in the injured sciatic nerve of celestrol-treated rats. These findings suggest that the phenotype of macrophages has a greater impact on regenerative outcomes than the total number of macrophages.

Real-time PCR

At two weeks postoperative, sciatic nerves were subjected to real-time PCR to assess the mRNA expression levels of BDNF and NGF. As shown in Figure 7, NGF and BDNF levels were significantly higher in both celestrol-treated groups than in controls (*P*<0.001). Furthermore, rats given 2 mg/kg celestrol had higher levels of BDNF expression than

rats given 1 mg/kg celestrol (*P*<0.001). Nevertheless, there was no significant difference in NGF mRNA expression between the two celestrol-treated groups. It should be noted that the mRNA level in naive rats was given a value of one.

ELISA assay

According to the result, inflammatory cytokine (TNF-α, IL-6, and IL-1β) levels were significantly lower in both celestrol groups when compared with the control group (Figure 8; *P*<0.001). Furthermore, rats given 2 mg/kg celestrol had significantly lower TNF-α (8.43 ± 1.3 pg/ml) than those given 1 mg/kg celestrol (18.61 ± 2.1 pg/ml), as shown in Figure 8A (*P*<0.001). IL-6 concentrations were

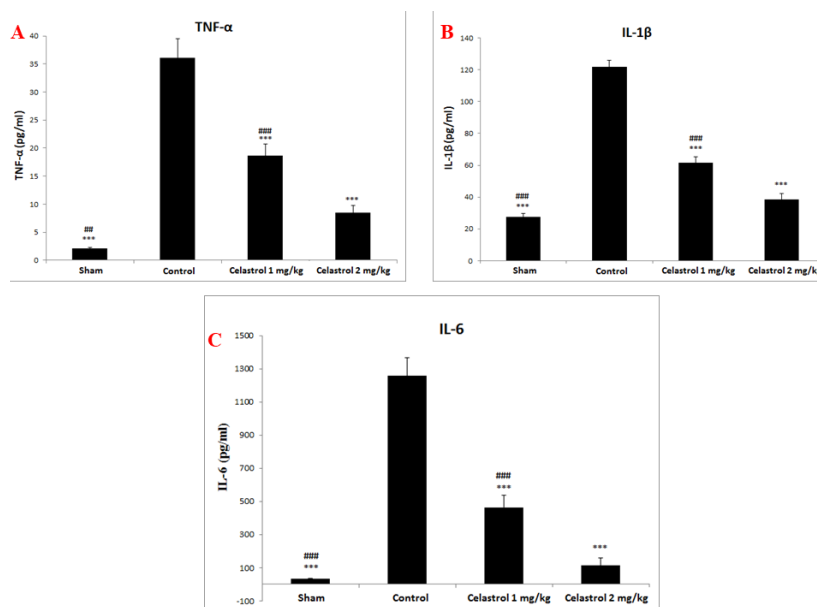


Figure 8. Neurotrophin levels in the sciatic nerve of rats treated with SNT. (A) TNF-α, (B) IL-1β, and (C) IL-6. The data are shown as mean ± SD (n = 4). ****P*<0.001 vs control group and ### *P*<0.001 vs celestrol (2 mg/kg) group

also significantly lower in the 2 mg/kg celastrol group (114 ± 43 pg/ml) compared with the 1 mg/kg celastrol group (463 ± 76 pg/ml) (Figure 8C; $P < 0.001$). Finally, celastrol treatment reduced IL-1 β levels from 61.4 ± 4.1 pg/ml at dose of 1 mg/kg to 38.6 ± 3.7 pg/ml at 2 mg/kg celastrol treatment (Figure 8B; $P < 0.001$). These findings suggested that celastrol has anti-inflammatory properties.

Discussion

Celastrol is a natural compound with anti-inflammatory and macrophage phenotype modulation properties which has been widely used in traditional Chinese medicine (41). Celastrol's therapeutic effects have been studied in a variety of disorders, including cancer, neuropathic pain, cerebral ischemia, traumatic brain injury (TBI), and chronic neurodegenerative disorders (42). However, the protective effect of celastrol on PNI is unknown. We looked at the neuroprotective effects of celastrol (1 or 2 mg/kg) in a rat SNT model. These doses were chosen based on previous research. Our findings suggest that two weeks of celastrol treatment immediately following an SNT could improve sciatic nerve regeneration and sensorimotor restoration significantly. Walking track analysis and hotplate tests consistently revealed sensorimotor impairment in the control group up to 16 weeks after surgery, but celastrol treatment improved sensorimotor dysfunction. According to electrophysiological and gastrocnemius muscle weight analysis, celastrol treatment facilitated motor nerve regeneration and significantly improved functional recovery after PNI. Histological analysis revealed that celastrol-treated rats had more axons extended along with the distal nerve stump. The initial increase in the number of axons distal to the site of transection has been shown to last for six months. Over the next two years, the number of axons gradually declines to pre-transection levels (43). These significant effects were observed in both the 1 mg/kg and 2 mg/kg doses of celastrol, although the 2 mg/kg dose was superior to the 1 mg/kg dose. However, because we only administered two doses of celastrol, the greater neuroprotective effects of the 2 mg/kg celastrol compared with the 1 mg/kg celastrol cannot be interpreted as dose-dependent. Moreover, since celastrol has a narrow therapeutic window due to toxicity at high doses, we did not use higher doses of celastrol in the current study (44).

According to our findings, celastrol can promote nerve regeneration by altering macrophage polarization toward pro-healing phenotypes (M2a and M2c), lowering pro-inflammatory cytokine release, and potentiating anti-inflammatory cytokine production. Increased BDNF secretion following celastrol treatment, on the other hand, is an important factor in nerve regeneration enhancement. Other studies have shown that BDNF treatment can improve survival and neurite sprouting while also stabilizing synapses and regulating neuroplasticity in PNI. Additionally, BDNF could reduce proinflammatory cytokine (TNF- α , IL-1 β , and IL-6) secretion but not mRNA expression in macrophages (45). Moreover, there is no significant difference in NGF mRNA expression between 1 and 2 mg/kg celastrol-treated rats. NGF affects the survival and maturation of sensory neurons and induces axonal sprouting. This finding may explain why there was no statistically significant difference in sensory function recovery or axon diameter between the two celastrol treatment groups (46). However, more research will be required in the future to confirm this. It's worth

mentioning that we assessed neurotrophin expression two weeks after surgery because prior studies have shown that neurotrophin expression in rodent neurons peaks seven days after injury, remains high until the 14th day, and then returns to baseline by the 30th day (47, 48). Furthermore, the phenotype of macrophages was evaluated three weeks after surgery because studies have shown that macrophage numbers at the site of nerve injury peak 14-21 days after a PNI (14, 49). In addition, since studies have shown a significant increase in the secretion of IL-6, TNF- α , and IL-1 β during the first week following PNI, we evaluated these cytokines as classical activators of the M1 phenotype of macrophages in the 1st-week post-surgery (50).

Several studies have found that both macrophage phenotypes are required for proper neural regeneration, but prolonged M1 macrophage activation within the lesion site has been linked to increased inflammatory cytokine secretion, nerve growth decline, and necrosis. For example, Mokarram *et al.* (2012) discovered a linear relationship between the ratio of pro-healing to pro-inflammatory macrophages (M2/M1) and the axon count at the distal nerve stump in a study that investigated the effect of macrophage phenotype in a rat model of PNI. They polarize macrophages toward M1 or M2 phenotypes by delivering IFN- γ or IL-4 locally within a polymeric scaffold that fills a 15 mm sciatic nerve gap. Their findings showed that initial macrophage polarization toward the M2a and M2c phenotypes facilitated Schwann cell infiltration and stimulated axonal regeneration. They concluded that the CD206+/CCR7+ macrophage ratio is associated with the ultimate regeneration outcome three weeks after surgery (14). In spinal cord injury, however, macrophage polarization toward the M2 phenotype does not occur, which could prevent appropriate neural regeneration. In this regard, Kuo *et al.* (2011) in a rat model of spinal cord injury found that polarizing macrophages toward the M2 phenotype with acid fibroblast growth factor (aFGF) enhanced neurotrophin production and, as a result, axonal regeneration (51).

Several studies, on the other hand, were conducted to investigate the neuroprotective effects of celastrol therapy against peripheral nerve injury. Previous work by Yang *et al.* (2014) demonstrated that intraperitoneal administration of 0.3 mg/kg celastrol resulted in significant analgesic and anti-neuropathic pain effects in mice with spared nerve injury (SNI). Results revealed celastrol reduced mRNA expressions of inflammatory cytokines, TNF- α , IL-6, and IL-1 β in SNI mic. They concluded that the analgesic effect of celastrol was mediated through cannabinoid receptor-2 (CB2) signaling (14, 25). In another study, Kyung *et al.* (2015) found that celastrol (1 mg/kg/IP) treatment improved the survival of retinal ganglion cells (RGCs) in a rat model of optic nerve crush. They explained that the mechanisms underlying celastrol's RGC protection are related to TNF- α mediated cell death inhibition (21).

Several experiments have also shown that celastrol treatment protects against CNS diseases. For example, Dai *et al.* (2019) investigated the anti-inflammatory and neuroprotective effects of celastrol (1 mg/kg/IP) on the pyroptosis pathway following acute spinal cord injury in rats. Pyroptosis is a type of apoptosis that is closely associated with inflammation. Their findings demonstrated that celastrol could reduce the inflammatory response after spinal cord injury by inhibiting microglial activation and the

pyroptosis pathway. These effects resulted in a decrease in the spinal cord cavity and neuronal loss (52). Another study, conducted by Jiang *et al.* (2018), discovered that celastrol (1 mg/kg/IP) treatment had protective effects against ischemic stroke, most likely through increasing IL-33/ST2-mediated polarization of microglia/macrophage M2. IL-33 is an IL-1 family member that induces macrophage polarization toward the pro-healing M2 phenotype when released by damaged or necrotic epithelial cells (18). Furthermore, Zhang *et al.* (2020) demonstrated in a rat model of transient global cerebral ischemia-reperfusion that celastrol (1, 2, or 4 mg/kg/IP) could reduce the secretion of proinflammatory cytokines such as TNF- α , IL-1b, and IL-6 while significantly increasing the anti-inflammatory marker IL-10 by inhibiting the HMGB1/NF- κ B signaling pathway. The transcription factor NF- κ B is linked to inflammation, oxidative stress, and apoptosis. Furthermore, celastrol reduced ischemia-induced oxidative stress while increasing anti-oxidant markers. Celastrol also reduced apoptotic neuronal death in the hippocampus and improved ischemia-induced neurological deficits (53). In another experiment, Liu *et al.* (2021) demonstrated that celastrol has neuroprotective and anti-inflammatory effects in the oxygen-glucose deprivation (OGD) model in primary rat cortical neuron culture. Besides, they showed that systemic injection of celastrol at doses of 1 and 6 mg/kg could protect against neural injuries caused by middle cerebral artery occlusion (MCAO). They determined that celastrol provided neuroprotective and anti-inflammatory effects by selectively binding to high mobility group protein 1 (HMGB1) and targeting the HSP70 and NF- κ B pathways (54). Similarly, Chen *et al.* (2022) investigated the neuroprotective effects of celastrol against cerebral ischemia/reperfusion damage in a mouse model of temporary middle cerebral artery closure. They proposed that celastrol protects against cerebral ischemia/reperfusion damage by suppressing glycolysis via the HIF-1 α /PDK1 axis (22).

Despite demonstrating the efficacy of celastrol treatment in peripheral nerve regeneration, there are several limitations to this study. First, we did not evaluate the celastrol effects on neural apoptosis, neurogenesis, and neuroplasticity. Furthermore, the celastrol impact on Schwann cells, which are significant in nerve regeneration, was not investigated. Finally, we did not look into the mechanisms of celastrol's neuroprotective effects on PNI. Future research should study the effects of celastrol on Schwann cells *in vivo* and *in vitro*. Moreover, the antioxidant properties of celastrol, as well as its potential ability to suppress apoptosis in neurons, should be investigated.

Conclusion

This study suggests that two weeks of intraperitoneal celastrol administration following an SNT and direct suture could improve the regeneration process and functional recovery. Celastrol appears to have neuroprotective properties due to immunomodulatory activity as well as regulatory effects on macrophage response to injury. However, more study is required to confirm these findings.

Acknowledgment

We thank Research Council of University of Mohaghegh Ardabili for financial support and Presidency of University of Al-Ameed.

Authors' Contributions

AA and HAG Conceived and designed the analysis. SMK, MBG, and HFA Collected the data and contributed data or analysis tools. AA, HFA, and HAG Performed the analysis and wrote the paper.

Conflicts of Interest

None.

References

- Scheib J, Höke A. Advances in peripheral nerve regeneration. *Nat Rev Neurol* 2013; 9:668-676.
- Abdolmaleki A, Zahri S, Bayrami A. Rosuvastatin enhanced functional recovery after sciatic nerve injury in the rat. *Eur J Pharmacol* 2020; 882:173260-173290.
- Magaz A, Faroni A, Gough JE, Reid AJ, Li X, Blaker JJ. Bioactive silk-based nerve guidance conduits for augmenting peripheral nerve repair. *Adv Healthc Mater* 2018; 7:1800308-1800328.
- Endo T, Kadoya K, Suzuki T, Suzuki Y, Terkawi MA, Kawamura D, *et al.* Mature but not developing schwann cells promote axon regeneration after peripheral nerve injury. *NPJ Regen Med* 2022; 7:1-11.
- Zhang K, Jiang M, Fang Y. The drama of wallerian degeneration: The cast, crew, and script. *Ann Rev Genet* 2021; 55:93-113.
- Bautista M, Krishnan A. Self-renewal of peripheral nerve resident macrophage: Does it represent a unique activation status? *Neural Regen Res* 2022; 17:999-1001.
- Li J, Yao Y, Wang Y, Xu J, Zhao D, Liu M, *et al.* Modulation of the crosstalk between schwann cells and macrophages for nerve regeneration: A therapeutic strategy based on multifunctional tetrahedral framework nucleic acids system. *Adv Mater* 2022; e2202513.
- Chen P, Piao X, Bonaldo P. Role of macrophages in wallerian degeneration and axonal regeneration after peripheral nerve injury. *Acta Neuropathol* 2015; 130:605-618.
- Li Y, Kang S, Halawani D, Wang Y, Alves CJ, Ramakrishnan A, *et al.* Macrophages facilitate peripheral nerve regeneration by organizing regeneration tracks through plexin-B2. *Genes Dev* 2022; 36:133-148.
- Zigmond RE, Echevarria FD. Macrophage biology in the peripheral nervous system after injury. *Prog Neurobiol* 2019; 173:102-121.
- Gaudet AD, Popovich PG, Ramer MS. Wallerian degeneration: Gaining perspective on inflammatory events after peripheral nerve injury. *J Neuroinflammation* 2011; 8:1-13.
- Stratton JA, Holmes A, Rosin NL, Sinha S, Vohra M, Burma NE, *et al.* Macrophages regulate schwann cell maturation after nerve injury. *Cell Rep* 2018; 24:2561-2572.
- Govindappa PK, Elfar JC. Erythropoietin promotes M2 macrophage phagocytosis of schwann cells in peripheral nerve injury. *Cell Death Dis* 2022; 13:1-12.
- Mokarram N, Merchant A, Mukhatyar V, Patel G, Bellamkonda RV. Effect of modulating macrophage phenotype on peripheral nerve repair. *Biomaterials* 2012; 33:8793-8801.
- Julier Z, Park AJ, Briquez PS, Martino MM. Promoting tissue regeneration by modulating the immune system. *Acta Biomaterialia* 2017; 53:13-28.
- Pei T, Yan M, Kong Y, Fan H, Liu J, Cui M, *et al.* The genome of tripterygium wilfordii and characterization of the celastrol biosynthesis pathway. *Gigabyte* 2021; 2021:1-32.
- Zhu Y, Zhang X, Zhang Y, Lü S, Li C. Identification of genes involved in celastrol biosynthesis by comparative transcriptome analysis in tripterygium wilfordii. *Phyton* 2022; 91:279-291.
- Jiang M, Liu X, Zhang D, Wang Y, Hu X, Xu F, *et al.* Celastrol treatment protects against acute ischemic stroke-induced brain injury by promoting an IL-33/ST2 axis-mediated microglia/

- macrophage M2 polarization. *J Neuroinflammation* 2018; 15:1-12.
19. Luo D, Guo Y, Cheng Y, Zhao J, Wang Y, Rong J. Natural product celastrol suppressed macrophage M1 polarization against inflammation in diet-induced obese mice via regulating Nrf2/HO-1, MAP kinase and NF- κ B pathways. *Aging (Albany NY)* 2017; 9:2069-2082.
 20. Wu M, Chen W, Yu X, Ding D, Zhang W, Hua H, et al. Celastrol aggravates LPS-induced inflammation and injuries of liver and kidney in mice. *Am J Transl Res* 2018; 10:2078-2086.
 21. Kyung H, Kwong JM, Bekerman V, Gu L, Yadegari D, Caprioli J, et al. Celastrol supports survival of retinal ganglion cells injured by optic nerve crush. *Brain Res* 2015; 1609:21-30.
 22. Chen M, Liu M, Luo Y, Cao J, Zeng F, Yang L, et al. Celastrol protects against cerebral ischemia/reperfusion injury in mice by inhibiting glycolysis through targeting HIF-1 α /PDK1 axis. *Oxid Med Cell Longev* 2022; 2022:1-14.
 23. Bernal J, Baldwin M, Gleason T, Kuhlman S, Moore G, Talcott M. Guidelines for rodent survival surgery. *J Invest Surg* 2009; 22:445-451.
 24. Mohammad-Bagher G, Arash A, Morteza B-R, Naser M-S, Ali M. Synergistic effects of acetyl-L-carnitine and adipose-derived stromal cells on improving regenerative capacity of acellular nerve allograft in sciatic nerve defect. *J Pharmacol Exp Ther* 2019; 368:490-502.
 25. Yang L, Li Y, Ren J, Zhu C, Fu J, Lin D, et al. Celastrol attenuates inflammatory and neuropathic pain mediated by cannabinoid receptor type 2. *Int J Mol Sci* 2014; 15:13637-13648.
 26. Kiaei M, Kipiani K, Petri S, Chen J, Calingasan NY, Beal MF. Celastrol blocks neuronal cell death and extends life in transgenic mouse model of amyotrophic lateral sclerosis. *Neurodegener Dis* 2005; 2:246-254.
 27. Bain J, Mackinnon S, Hunter D. Functional evaluation of complete sciatic, peroneal, and posterior tibial nerve lesions in the rat. *Plast Reconstr Surg* 1989; 83:129-138.
 28. Sarikcioglu L, Demirel B, Utuk A. Walking track analysis: An assessment method for functional recovery after sciatic nerve injury in the rat. *Folia morphol* 2009; 68:1-7.
 29. Ferdowsi S, Abdolmaleki A, Asadi A, Zahri S. Glibenclamide promoted functional recovery following sciatic nerve injury in male wistar rats. *Fundam Clin Pharmacol* 2022.
 30. Hargreaves K, Dubner R, Brown F, Flores C, Joris J. A new and sensitive method for measuring thermal nociception in cutaneous hyperalgesia. *Pain* 1988; 32:77-88.
 31. Rupp A, Dornseifer U, Fischer A, Schmahl W, Rodenacker K, Jütting U, et al. Electrophysiologic assessment of sciatic nerve regeneration in the rat: Surrounding limb muscles feature strongly in recordings from the gastrocnemius muscle. *J Neurosci Methods* 2007; 166:266-277.
 32. Scipio FD, Raimondo S, Tos P, Geuna S. A simple protocol for paraffin-embedded myelin sheath staining with osmium tetroxide for light microscope observation. *Microsc Res Tech* 2008; 71:497-502.
 33. Varejão AS, Melo-Pinto P, Meek MF, Filipe VM, Bulas-Cruz J. Methods for the experimental functional assessment of rat sciatic nerve regeneration. *Neurol Res* 2004; 26:186-194.
 34. Azimpour M, Mahmoudi F, Abdolmaleki A, Bayrami A. Thyroxine accelerates functional recovery in a rat model of sciatic nerve crush. *Turk Neurosurg* 2022; 32:298-304.
 35. Zhang X, Alwaal A, Lin G, Li H, Zaid UB, Wang G, et al. Urethral musculature and innervation in the female rat. *NeuroUrol Urodyn* 2016; 35:382-389.
 36. Soluki M, Mahmoudi F, Abdolmaleki A, Asadi A, Sabahi Namini A. Cerium oxide nanoparticles as a new neuroprotective agent to promote functional recovery in a rat model of sciatic nerve crush injury. *Br J Neurosurg* 2020; 186:4292:1-6.
 37. Clements IP, Kim Y-t, English AW, Lu X, Chung A, Bellamkonda RV. Thin-film enhanced nerve guidance channels for peripheral nerve repair. *Biomaterials* 2009; 30:3834-3846.
 38. Maeda Y, Otsuka T, Takeda M, Okazaki T, Shimizu K, Kuwabara M, et al. Transplantation of rat cranial bone-derived mesenchymal stem cells promotes functional recovery in rats with spinal cord injury. *Sci Rep* 2021; 11:1-11.
 39. Tirassa P, Manni L, Stenfors C, Lundeberg T, Aloe L. RT-PCR ELISA method for the analysis of neurotrophin mRNA expression in brain and peripheral tissues. *J Biotechnol* 2000; 84:259-272.
 40. Elfving B, Plougmann PH, Wegener G. Detection of brain-derived neurotrophic factor (BDNF) in rat blood and brain preparations using ELISA: Pitfalls and solutions. *J Neurosci Methods* 2010; 187:73-77.
 41. Astry B, Venkatesha SH, Laurence A, Christensen-Quick A, Garzino-Demo A, Frieman MB, et al. Celastrol, a Chinese herbal compound, controls autoimmune inflammation by altering the balance of pathogenic and regulatory T cells in the target organ. *Clin Immunol* 2015; 157:228-238.
 42. Zhang C, Zhao M, Wang B, Su Z, Guo B, Qin L, et al. The Nrf2-NLRP3-caspase-1 axis mediates the neuroprotective effects of celastrol in parkinson's disease. *Redox Biol* 2021; 47:102134-102149.
 43. MacKinnon SE, Dellon A, O'brien J. Changes in nerve fiber numbers distal to a nerve repair in the rat sciatic nerve model. *Muscle Nerve* 1991; 14:1116-1122.
 44. Bai X, Fu R-J, Zhang S, Yue S-J, Chen Y-Y, Xu D-Q, et al. Potential medicinal value of celastrol and its synthesized analogues for central nervous system diseases. *Biomed Pharmacother* 2021; 139:111551-111568.
 45. Yu H-C, Huang H-B, Huang Tseng H-Y, Lu M-C. Brain-derived neurotrophic factor suppressed proinflammatory cytokines secretion and enhanced microRNA (miR)-3168 expression in macrophages. *Int J Mol Sci* 2022; 23:570-585.
 46. Keefe KM, Sheikh IS, Smith GM. Targeting neurotrophins to specific populations of neurons: NGF, BDNF, and NT-3 and their relevance for treatment of spinal cord injury. *Int J Mol Sci* 2017; 18:548-565.
 47. Önger ME, Delibaş B, Türkmen AP, Erener E, Altunkaynak BZ, Kaplan S. The role of growth factors in nerve regeneration. *Drug Discov Ther* 2016; 10:285-291.
 48. Li R, Li D-h, Zhang H-y, Wang J, Li X-k, Xiao J. Growth factors-based therapeutic strategies and their underlying signaling mechanisms for peripheral nerve regeneration. *Acta Pharmacol Sin* 2020; 41:1289-1300.
 49. Shen ZL, Lassner F, Bader A, Becker M, Walter GF, Berger A. Cellular activity of resident macrophages during wallerian degeneration. *Microsurgery* 2000; 20:255-261.
 50. Büttner R, Schulz A, Reuter M, Akula AK, Mindos T, Carlstedt A, et al. Inflammation impairs peripheral nerve maintenance and regeneration. *Aging Cell* 2018; 17:12833-12848.
 51. Kuo H-S, Tsai M-J, Huang M-C, Chiu C-W, Tsai C-Y, Lee M-J, et al. Acid fibroblast growth factor and peripheral nerve grafts regulate Th2 cytokine expression, macrophage activation, polyamine synthesis, and neurotrophin expression in transected rat spinal cords. *J Neurosci* 2011; 31:4137-4147.
 52. Dai W, Wang X, Teng H, Li C, Wang B, Wang J. Celastrol inhibits microglial pyroptosis and attenuates inflammatory reaction in acute spinal cord injury rats. *Int Immunopharmacol* 2019; 66:215-223.
 53. Zhang B, Zhong Q, Chen X, Wu X, Sha R, Song G, et al. Neuroprotective effects of celastrol on transient global cerebral ischemia rats via regulating HMGB1/NF- κ B signaling pathway. *Front Neurosci* 2020; 14:847-864.
 54. Liu D-D, Luo P, Gu L, Zhang Q, Gao P, Zhu Y, et al. Celastrol exerts a neuroprotective effect by directly binding to HMGB1 protein in cerebral ischemia-reperfusion. *J Neuroinflammation* 2021; 18:1-18.